



Perspective Article

An NMR study of hydrofluorocarbon mixed-gas solubility and self-diffusivity in the ionic liquid 1-ethyl-3-methylimidazolium dicyanamide

Miguel Viar^a, Fernando Pardo^a, Gabriel Zarca^a, Leoncio Garrido^{b,*}, Ane Urtiaga^{a,*} 

^a Department of Chemical and Biomolecular Engineering, Universidad de Cantabria, Avda Los Castros 46, 39005 Santander, Spain

^b Department of Physical Chemistry of Polymers, Instituto de Ciencia y Tecnología de Polímeros (ICTP-CSIC), Juan de la Cierva 3, 28006, Madrid, Spain

ARTICLE INFO

Keywords:

R-32
R-125
R-410A
Ionic liquid
NMR
Mixture solubility
Self-diffusivity

ABSTRACT

To date, the design of advanced separation processes, such as the extractive distillation with ionic liquids (ILs), for the separation of common close-boiling refrigerant blends relies almost exclusively on binary equilibrium data obtained for single-gas/solvent systems, thus neglecting the influence of possible mixture effects. In this work, Nuclear Magnetic Resonance (NMR) spectroscopy and pulsed gradient spin echo (PGSE) NMR are proposed for the sequential assessment of the single and mixed-gas vapor-liquid equilibrium and self-diffusivity of two fluorinated refrigerants, difluoromethane (R-32) and pentafluoroethane (R-125), in the IL 1-ethyl-3-methylimidazolium dicyanamide at 303.1 K and pressures up to 4 bar, either as pure R-32 or using the commercial refrigerant blend R-410A. The results confirmed that the mixed-gas solubility and self-diffusivities were essentially equal to those obtained with pure feed gas, thus significant mixing effects were not observed for this particular system. However, an increase in the self-diffusion coefficients was observed with the concentration of absorbed gas, which was more significant for the smallest hydrofluorocarbon (R-32) than for R-125. This technique also allowed evaluating the mobility of the IL moieties, which was slightly higher for the IL anion. Moreover, the self-diffusion coefficients of the IL ions also increased with the amount of gas absorbed, yet less markedly than for the refrigerants. Overall, the NMR technique proved to be an accurate method for the rapid screening of possible mixture effects in equilibrium and transport properties of refrigerant and IL systems, thus providing essential information for designing novel advanced separation processes.

1. Introduction

The refrigeration, air conditioning and heat pump (RACHP) sector is facing an urgent need to develop sustainable solutions to reduce its greenhouse gas emissions [1]. In response to the implementation of international agreements, such as the Kigali Amendment to the Montreal Protocol, the sector is urged to reduce significantly the global emissions of hydrofluorocarbons (HFCs) into the atmosphere [2,3]. HFCs are the third generation of refrigerants that, despite not being ozone depleting substances, exhibit a high global warming potential (GWP), which can be up to 12,000 times higher than that of carbon dioxide [4,5]. This characteristic renders them a priority target in global climate change mitigation policies [6]. In this context, current research is focused on two main approaches: (i) the development of new refrigerants and formulation of novel blends with much lower GWP [7,8] and (ii) the

implementation of advanced processes for the recovery and recycling of HFCs at the end of life of the refrigeration equipment [9,10]. Regarding the latter approach, extractive distillation with ionic liquids (ILs) emerged as a promising technology due to its ability to efficiently separate HFC-blends with close boiling points [11–13]. Thus, the solubility of single HFCs has been extensively investigated in assorted ILs employing experimental methods [14–17] as well as computational tools such as machine learning [18,19], quantum chemistry [20–22], and molecular simulations [23,24].

In contrast, the influence of mixed-gas solubility of HFCs in ILs, a highly valuable knowledge for process design, has received less attention to date. This is likely due to the difficulty and cost of applying the experimental and analytical techniques required for analysing the solubility of multicomponent gas mixtures. It was only recently that Baca et al. [25] reported a new methodology incorporating the Integral Mass

* Corresponding authors.

E-mail addresses: garrido@ictp.csic.es (L. Garrido), urtiaga@unican.es (A. Urtiaga).

<https://doi.org/10.1016/j.fluid.2025.114340>

Received 8 November 2024; Received in revised form 9 January 2025; Accepted 15 January 2025

Available online 16 January 2025

0378-3812/© 2025 The Authors. Published by Elsevier B.V. This is an open access article under the CC BY-NC-ND license (<http://creativecommons.org/licenses/by-nc-nd/4.0/>).

Balance (IMB) method to a gravimetric microbalance for the measurement of the solubility of gas mixtures in ILs. They reported for the first time solubility values of different HFC mixtures of difluoromethane (R-32) and pentafluoroethane (R-125) in classical ILs such as 1-butyl-3-methylimidazolium tetrafluoroborate ($[\text{C}_4\text{C}_1\text{im}][\text{BF}_4]$) and 1-butyl-3-methylimidazolium hexafluorophosphate ($[\text{C}_4\text{C}_1\text{im}][\text{PF}_6]$). Similarly, gaining deeper insight into the diffusivity coefficients of mixed HFCs in ILs is essential for the accurate estimation of mass transfer rates in the extractive distillation process [9,10]. In this sense, recent works demonstrated that equilibrium models overestimate the process separation performance, a shortcoming that becomes particularly relevant for viscous ILs [11,26]. To date, the solubility and Fickian (non-equilibrium) diffusion of pure HFCs in ILs have been mostly measured using the isochoric saturation method, which allows the determination of diffusion coefficients at infinite dilution applying the semi-infinite volume model [17,27–29], and with microgravimetric balances that allow measuring the diffusion coefficients as a function of the concentration of absorbed gas [15,30,31]. Again, there is a missing gap regarding the influence of multicomponent HFC mixtures on the diffusivity of the absorbed species.

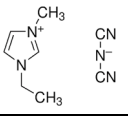
As stated above, the measurement of transport phenomena in multicomponent systems with macroscopic methods is often difficult to implement and provides limited knowledge on the behaviour of each component. To circumvent this problem, microscopic methods affording information at the molecular scale could be advantageous. Nuclear Magnetic Resonance (NMR) spectroscopy is a versatile and widely used technique in many different scientific fields to investigate the molecular structure and dynamics due to its sensitivity to the environment of the observed nuclei. Therefore, it is feasible with multinuclear NMR methods to identify and quantify simultaneously individual components in a mixture, providing that well resolved spectra are acquired. For example, in a related application to the problem at hand (i.e., separation of gas mixtures), Garrido et al. [32] used ^{13}C and ^1H NMR spectroscopy to determine the solubility coefficients of several neat and mixed gases in polymers. The application of NMR to research in ILs has been reviewed recently [33]. In addition, pulsed gradient spin echo (PGSE) NMR methods, also known as PFG NMR, allow the assessment of molecular dynamics in many diverse systems. After the initial works by Stejskal and Tanner [34] reporting the measurement of diffusion coefficients with the PGSE NMR method, numerous applications in different fields of research have been shown. In particular, this method has been used in electrochemistry to investigate ions transport mobility in ILs in combination with conductivity measurements [35–37]. Overall, the NMR diffusion methodology has been described and reviewed profusely. The readers interested in wider scope are referred to thorough works on the subject [38–40]. Regarding the field of refrigerant gases-ILs, there are only two pioneering works. First, Ahooseini et al. [41] measured the self-diffusivity of 1,1,1,2-tetrafluoroethane (R-134a) in 1-hexyl-3-methylimidazolium bis(trifluoromethylsulfonyl)imide at different temperatures using the NMR tool. Also, Wang et al. [24] validated the diffusion coefficients of R-32 and R-125 in $[\text{C}_4\text{C}_1\text{im}][\text{BF}_4]$ predicted by molecular dynamics with NMR-experimental data.

Consequently, the combination of multinuclear spectroscopy and PGSE NMR enables the sequential determination of the molecular transport coefficients, solubility and diffusion, of multicomponent mixtures in a given medium or, in other words, the characterization of the medium transport properties, as it has been shown for, e.g., liquids and polymer membranes [42,43]. With this background, the aim of this work is to determine the solubility and self-diffusion coefficients of neat R-32 and of its equimass mixture with R-125 (known as R-410A) in the IL 1-ethyl-3-methylimidazolium dicyanamide ($[\text{C}_2\text{C}_1\text{im}][\text{dca}]$) with the NMR methods outlined above, and assess the soundness of the NMR as a viable approach to characterize the transport phenomena of fluorinated gases and, in particular, mixed gases in ILs. The IL $[\text{C}_2\text{C}_1\text{im}][\text{dca}]$ was selected for this study because of its low-viscosity and excellent solubility selectivity for the separation of these HFCs [17].

Table 1
Chemicals used in this work.

| Chemical | Formula | CAS No. | Fraction purity | Purification method | Water content |
|---|--|--------------|-----------------|---------------------|---------------|
| $[\text{C}_2\text{C}_1\text{im}][\text{dca}]$ | $\text{C}_8\text{H}_{11}\text{N}_5$ | 666,823–18–3 | >98 wt % | Vacuum dry | < 100 ppm |
| R-32 | CF_2H_2 | 75–10–2 | >99.9 vol % | – | – |
| R-410A | $\text{CF}_2\text{H}_2 + \text{CF}_3\text{CF}_2\text{H}$ (50/50 wt %) | 133,023–17–3 | >99.9 vol % | – | – |

Table 2
Main properties of the IL $[\text{C}_2\text{C}_1\text{im}][\text{dca}]$ [44–46].

| Chemical structure | |
|---|--------|
|  | |
| Molecular weight/g mol ⁻¹ | 177.21 |
| Melting temperature/K | 267.80 |
| Density at 303.1 K/kg m ⁻³ | 1098.5 |
| Viscosity at 303.1 K/mPa s | 12.7 |

2. Experimental section

2.1. Materials

The HFC R-32 and the R-410A refrigerant mixture were provided by Coproven Climatización (Gas Servei licensed supplier, Spain). R-410A is an equimass mixture of R-32 and R-125, where the molar percentage of each gas are 69.8/30.2 mol %, respectively. The IL $[\text{C}_2\text{C}_1\text{im}][\text{dca}]$ was supplied by IoLiTec (Germany) with a purity of 98 wt %. It was subjected to a 24-hour vacuum drying at 333.15 K to remove any traces of water prior to its use. The chemical specifications of the system components are summarized in Table 1. The final water content of the IL was measured to be <100 ppm using a coulometric Karl-Fischer titration method (899 Coulometer, Metrohm). Table 2 reports the main properties of the IL.

2.2. NMR solubility and diffusion measurements

The NMR measurements were performed in a Bruker Avance Neo 400 spectrometer (Bruker BioSpin GmbH, Rheinstetten, Germany) equipped with an 89 mm wide bore, 9.4 T superconducting magnet (^1H , ^{13}C and ^{19}F Larmor frequencies at 400.14, 100.61 and 376.51 MHz, respectively). To perform the NMR measurements of the fluorinated gases (F-gases), R-32 and R-410A, a weighted amount (~ 0.2 g) of the dried IL was injected in a 5 mm o.d. NMR tube with a valve designed for NMR studies of moderately pressurized gases (<6 bar), the valve was closed and the tube connected to a high vacuum line. The sample size (height ~ 15 mm) was chosen to fit within the active volume of the radiofrequency and gradient coils with the highest homogeneity of the respective fields. The volume of gas put in contact with the IL was 38 cm³, which guaranteed that the amount of F-gases absorbed is much lower (<5 %) than the total gas feed. Before filling the tube at a given pressure with a F-gas, the IL sample was cooled down below the reported melting temperature (to approximately 200 K) until solidification, degassed (high vacuum, < 10⁻⁵ bar), and followed by raising the temperature up to 298 K. This procedure was repeated three times to assure that air was completely removed from the sample before loading the gas or gases of interest. During the last cycle, the valve was kept open to the high vacuum line until the sample thawed completely and a temperature of 298 K was reached. This sample preparation method was proofed to be essential to guarantee the adequate F-gas absorption, compared to the

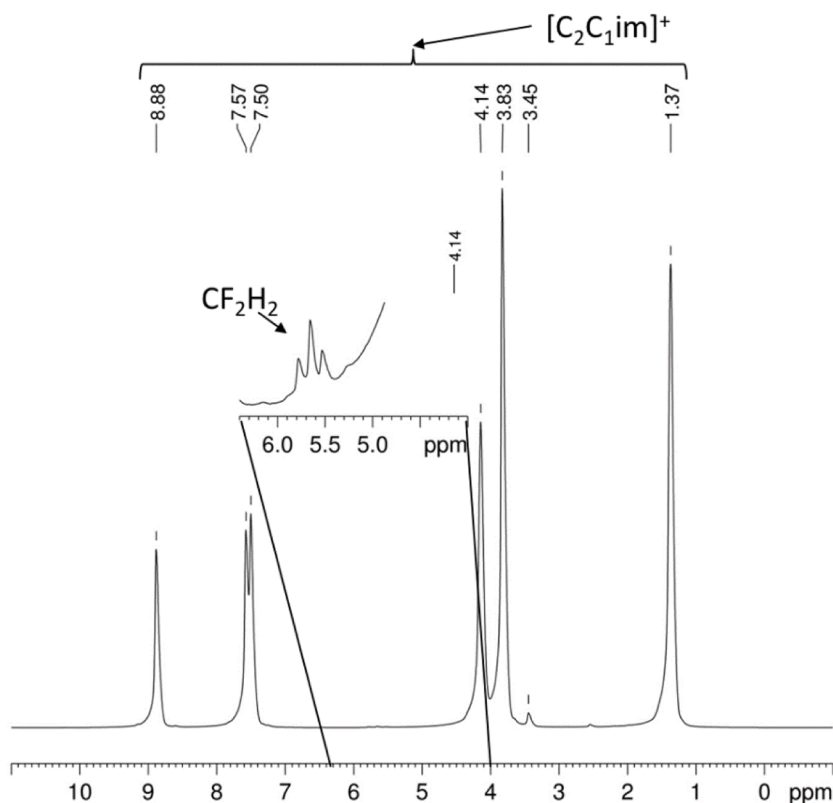


Fig. 1. ^1H NMR spectrum corresponding to a sample of $[\text{C}_2\text{C}_1\text{im}]^+$ [dca] (210 mg) with R-32 (p : 0.6 bar at 303.1 K). The inset shows a magnification of the proton signal at 5.66 ppm corresponding to the fluorinated gas.

initial assays in which IL degasification was performed at room temperature. The total gas pressure used in these experiments was varied between 0.5 and 5 bar to facilitate the measurements with adequate signal-to-noise ratio in a reasonable amount of time. The gas pressure was monitored with a transducer working in the range 0 – 10 bar.

The ^{13}C and ^{19}F T_1 relaxation measurements of the IL and sorbed gases were performed using a Bruker diffusion probehead Diff50 with two inserts (^{13}C and ^{19}F) for 5 mm o.d. NMR tubes, at 303.0 ± 0.1 K. The T_1 s of samples (IL and sorbed gases) were measured using an inversion-recovery (IR) pulse sequence. The solubility of gases in the IL was measured using an inversion-recovery pulse sequence to acquire the ^{19}F NMR spectra of samples with a repetition rate $\geq 5 \times T_1$. The value of inversion time, T_i , was chosen to null the contribution of free gas to the NMR signal. A standard consisting of a sealed glass capillary with a known amount of trifluoroacetic acid was used as external reference, and the ^{19}F NMR spectra were referenced to its ^{19}F chemical shift (-77.0 ppm), secondary to trichlorofluoromethane (0.0 ppm). For each spectrum, the individual gas peak areas were measured, corrected for the signal intensity reduction due to T_i , and normalized to the corresponding peak area of the standard. In the case of ^{13}C NMR, the external reference was a standard consisting of a sealed glass capillary with a known amount of labelled $^{13}\text{C}(1)$ acetic acid (178.1 ppm), secondary to tetramethylsilane (TMS, 0.0 ppm). The proton NMR spectra of the samples studied were dominated by the strong signals associated to the cation of the IL, as illustrated in Fig. 1. The intensity of the proton NMR signal of the sorbed R-32, centred at 5.66 ppm, was very small. This problem would be magnified when studying the sorption and diffusion of R-410A, due to partial overlap of the proton signals of R-32 and R-125 and low solubility of R-125. Overall, the ^1H NMR measurements of solubility of both gases in the IL were not feasible and the uncertainty of the ^1H PGSE NMR measurements in the case of R-32 was high. These limitations were overcome with ^{19}F NMR.

The samples prepared as described above were used to determine the

diffusion coefficients of sorbed neat and mixed gases using ^{13}C and ^{19}F NMR. For these measurements, a pulsed gradient stimulated spin echo sequence was used [47,48]. The echo time between the first two 90° rf pulses, τ_1 , was 2.1 ms. The self-diffusion coefficient of each gas, D , was measured at a diffusion time, t_D , of 22 ms. The length of the field gradient pulses, δ , was 1.0 ms. All time parameters were kept constant and only the amplitude of the gradient pulses varied from a small value up to a maximum of 11 T m^{-1} . The repetition rate was $\geq 5 \times T_1$, and the total acquisition time ranged from about 1 to 17 h. The diffusion coefficients were calculated by fitting the data to the well-known expression [34],

$$S(g) = S(0) \exp \left[-(\gamma \delta g)^2 \left(t_D - \frac{\delta}{3} \right) D \right] \quad (1)$$

where $S(g)$ and $S(0)$ represent the echo intensity in the presence of a gradient with amplitude g and 0, respectively; g is the gyromagnetic ratio of the nuclei being observed and D is the diffusion coefficient. When the measurement of D is made varying only the gradient amplitude g , there is not a need to consider the contribution of the T_1 and T_2 relaxation times terms to the signal attenuation. Prior to these measurements, the temperature at the sample volume in the probe head and the field gradient were calibrated as described previously [49].

3. Results and discussion

3.1. Single-gas and mixed-gas solubility

All NMR measurements were performed at thermodynamic equilibrium at 303.1 K. This condition was assessed by measuring the concentration of sorbed gas in the IL at increasing time after loading the gas, until a constant value was reached (24 h, approximately). As mentioned above, NMR allows the identification of different chemical moieties in a sample due to the sensitivity of the technique to the surroundings of the

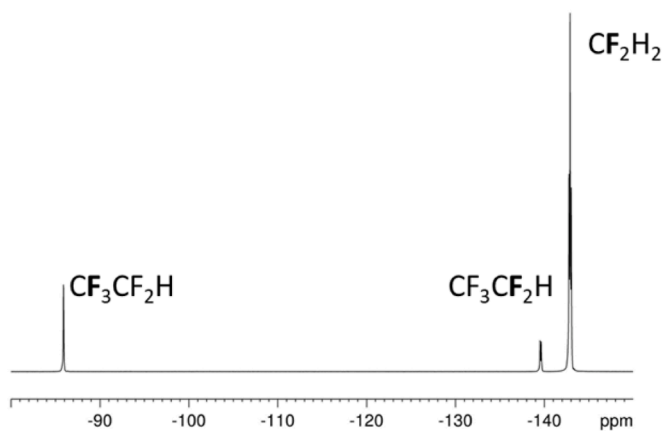


Fig. 2. ^{19}F NMR spectrum, without decoupling, corresponding to a sample of $[\text{C}_2\text{C}_1\text{im}][\text{dca}]$ (202 mg) at thermodynamic equilibrium with R-410A (3.81 bar) at 303.1 K. The peaks centered at -142.9 (t) ppm correspond to R-32, and the peaks at -139.6 (d) and -85.9 ppm correspond to R-125 ($\text{CF}_3\text{CF}_2\text{H}$). The nucleus of the chemical moiety associated to each peak is shown in bold.

nucleus of interest. Thus, if a well resolved spectrum of a multicomponent sample is obtained, it is feasible to characterize the behaviour of its components. In Fig. 2, an example of a ^{19}F NMR spectrum corresponding to the absorption of mixture R-410A in $[\text{C}_2\text{C}_1\text{im}][\text{dca}]$ is illustrated. In Fig. 3, the ^{13}C spectrum of the IL in the sample is shown. The spectral signatures of cation and anion carbons were well resolved, and this enabled the measurement of their corresponding diffusion coefficients.

The values of ^{19}F T_1 relaxation times of the sorbed gases, neat or mixed, in the IL did not vary significantly within the range of pressure studied and they were in the vicinity of 3.0 s for R-410A and 3.5 s for R-32. The values of ^{19}F T_1 s measured for the free gases were two orders of magnitude smaller, varying from 10 to 22 ms. Likewise, the ^{13}C T_1 relaxation times of the IL did not vary with the sorption of gases and their values for the cation carbons *d*, *e* and *f* (see labels in Fig. 3) were 1.44 s and for the anion (120.0 ppm) 6.64 s. The carbons of the sorbed gases were not observed because, with the conditions used in these experiments, their concentrations ($5.6 \cdot 10^{-4}$ M) were below the ^{13}C detection limit.

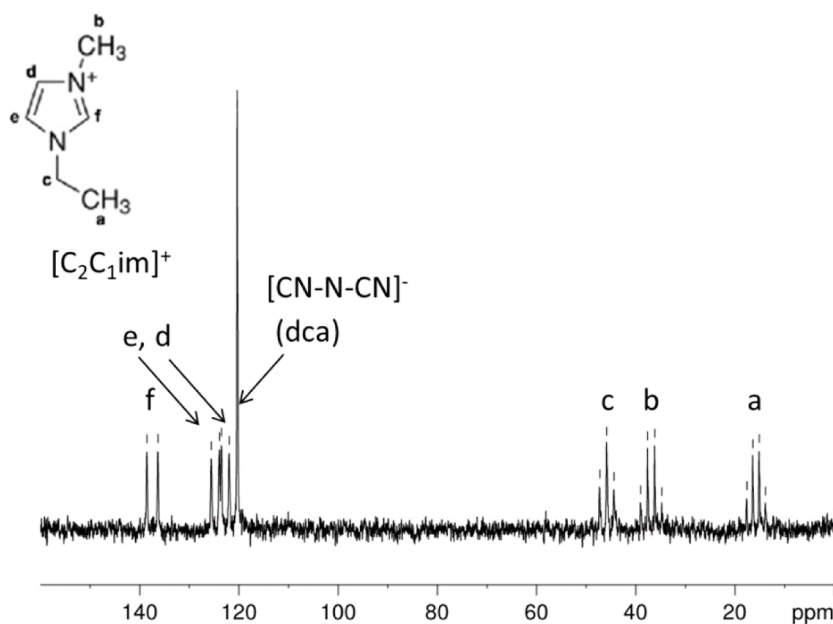


Fig. 3. ^{13}C NMR spectrum, without decoupling, corresponding to a sample of $[\text{C}_2\text{C}_1\text{im}]^+[\text{dca}]^-$ (202 mg) at thermodynamic equilibrium with R-410A (3.81 bar) at 303.1 K. The peaks labelled from *a* to *f* correspond to the carbons indicated in the cation (inset) and the peak at 120.0 ppm to the anion carbons.

The solubility measurements at pressures between 0.66 and 3.63 bar of the neat R-32 and R-32 mixed with R-125 are summarized in Tables 3 and 4, respectively. The differences between the ^{19}F chemical shifts of the two gases and in the relaxation times of the free and sorbed gases, enabled the determination of the solubility of each component in the IL.

The vapor-liquid equilibrium (VLE) data presented in Table 3 are also depicted in Fig. 4a, where the NMR solubility data of R-32 in $[\text{C}_2\text{C}_1\text{im}][\text{dca}]$ at different pressures are plotted together with the solubility data obtained with the isochoric saturation (IS) method in our previous study [28]. Both sets of data followed the same trend showing the adequacy and accuracy of the experimental procedure followed in the present study for determining the solubility of HFCs in ILs with the NMR technique.

Table 3

Solubility data of pure R-32 in $[\text{C}_2\text{C}_1\text{im}][\text{dca}]$ at 303.1 K.^a

| $P_{\text{R-32}}/\text{bar}$ | $x_{\text{R-32}}$ |
|------------------------------|-------------------|
| 0.66 | 0.0210 |
| 1.62 | 0.0513 |
| 2.45 | 0.0744 |
| 3.63 | 0.1157 |

^a Standard uncertainties *u* are $u(T) = 0.1$ K, $u(P) = 0.01$ bar, and $u(x) = 0.05x$.

Table 4

Mixed-gas solubility data of the R-410A blend (R-32 and R-125, 69.8/30.2 mol %) in $[\text{C}_2\text{C}_1\text{im}][\text{dca}]$ at 303.1 K.^a

| $P_{\text{R-410A}}/\text{bar}$ | $x_{\text{R-410A}}$ | $P_{\text{R-32}}/\text{bar}$ | $x_{\text{R-32}}$ | $P_{\text{R-125}}/\text{bar}$ | $x_{\text{R-125}}$ |
|--------------------------------|---------------------|------------------------------|-------------------|-------------------------------|--------------------|
| 0.93 | 0.0229 | 0.64 | 0.0212 | 0.29 | 0.0017 |
| 1.73 | 0.0417 | 1.19 | 0.0385 | 0.54 | 0.0032 |
| 2.51 | 0.0629 | 1.72 | 0.0579 | 0.79 | 0.0050 |
| 3.81 | 0.0902 | 2.62 | 0.0825 | 1.19 | 0.0077 |

^a Standard uncertainties *u* are $u(T) = 0.1$ K, $u(P) = 0.01$ bar, and $u(x) = 0.05x$.

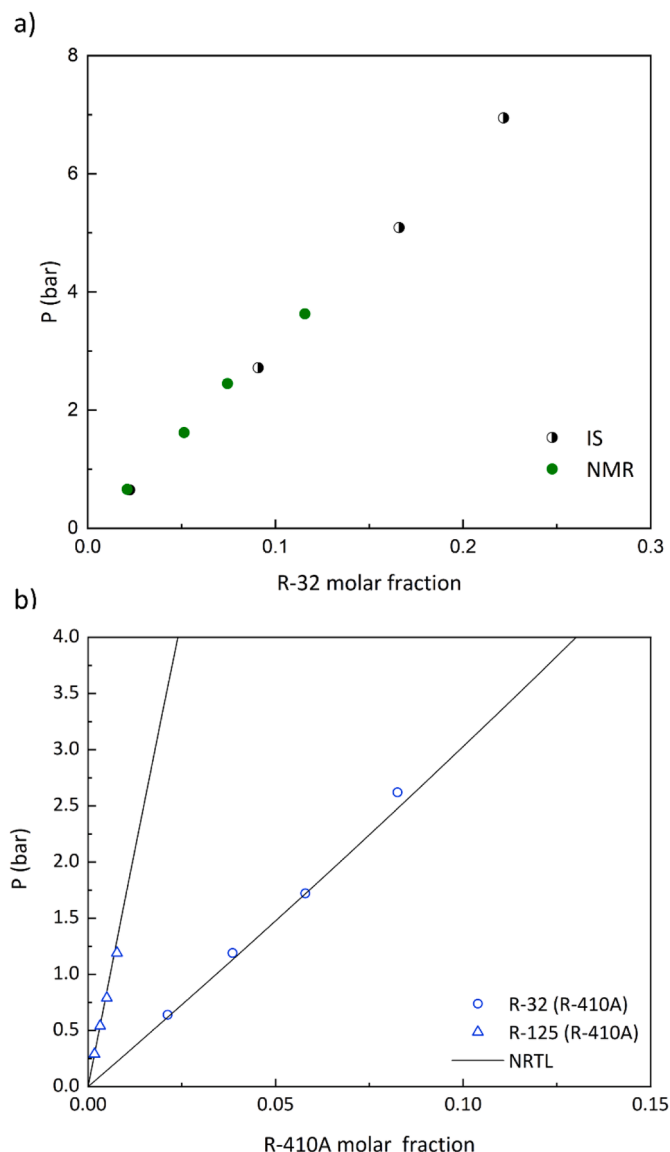


Fig. 4. a) VLE between neat R-32 and $[C_2C_1im][dca]$ obtained with the NMR technique (filled circles) and the IS method (half-filled circles) [28]. b) Multi-component VLE between R-32 (empty circles) + R-125 (empty triangles) and $[C_2C_1im][dca]$ measured by NMR (feed composition: R-410A mixture). Solid lines represent the VLE results obtained with the NRTL model for pure R-32 and R-125 [28]. All data obtained at 303.1 K.

Fig. 4b presents the mixed-gas solubility data of R-32 and R-125, using the R-410A blend as feed gas, together with the predictions of the NRTL model reported by Asensio et al. [28] for the absorption in $[C_2C_1im][dca]$ of pure R-32 and R-125. The deviation between the NRTL model and the NMR mixed-gas absorption data was quantified in terms of the average absolute relative deviation (AARD), which was calculated with Eq. (2).

$$AARD = \frac{100}{N} \sum_{i=1}^N \left| \frac{y_{NRTL_i} - y_{NMR_i}}{y_{NMR_i}} \right| \quad (2)$$

No significant mixture effects were observed in the R-32 and R-125 solubility as the experimental mixed-gas equilibrium data were closely aligned with the NRTL model derived for the individual compounds. The AARD of the NRTL model with respect to the NMR mixed-gas solubility data of R-32 and R-125 were 2.90 and 4.20%, respectively. Also, the results obtained were consistent with those reported by Baca et al. [25]

Table 5

Self-diffusivity of R-32 in $[C_2C_1im][dca]$ at 303.1 K and several pressures.^a

| P/bar | $D/10^{-10} \text{ m}^2 \text{ s}^{-1}$ | $u(D)$ |
|----------------|---|--------|
| 0.66 | 4.47 | 0.06 |
| 1.62 | 4.75 | 0.02 |
| 2.45 | 5.02 | 0.03 |
| 3.63 | 5.43 | 0.05 |

^a Standard uncertainties u are $u(T) = 0.1 \text{ K}$ and $u(P) = 0.01 \text{ bar}$.

for different ILs, who found that the single absorption of R-32 and R-125 were mostly equal to the mixed R-32/R-125 solubility in $[C_4C_1im][PF_6]$ and $[C_4C_1im][BF_4]$ using the previously mentioned IMB method. Accordingly, it could be concluded that the use of VLE models independently derived for the individual components of the R-410A mixture is a suitable strategy for the design of advanced separation processes with these imidazolium-based ILs. Moreover, the NMR technique can be regarded as a valuable tool in the early stages of process design to confirm or discard with fast and reliable measurements whether other systems, particularly more viscous ILs, exhibit significant competitive or synergistic mixing effects.

3.2. F-gas self-diffusivity

The self-diffusivity of neat R-32 sorbed in the IL $[C_2C_1im][dca]$ was measured at 303.1 K across a pressure range up to 4 bar. Moreover, the PGSE-NMR technique allowed simultaneously measuring, for the first time, the R-32 and R-125 self-diffusivities in $[C_2C_1im][dca]$ under mixed-gas conditions using the R-410A blend as feed gas. In both cases, the measurements were performed under equilibrium conditions between the two phases. The results of the ^{19}F diffusion measurements of neat R-32 and mixed R-32 with R-125 in $[C_2C_1im][dca]$ are summarized in Tables 5 and 6, respectively. As can be seen in Table 6, the self-diffusivity of the smallest molecule (R-32) almost doubled that of R-125, which would also contribute to ease their separation by extractive distillation under a kinetic-control regime.

Fig. 5 illustrates the self-diffusivity results as a function of the mole fraction of gas absorbed in the IL, either R-32 or the sum of mol fractions of R-32 and R-125 (please check the relation between pressure and gas absorption data in Tables 3 and 4). As can be seen, the R-32 self-diffusivity was not influenced by the feed source, which reflected (as for the solubility) the absence of positive or negative mixing effects on the transport properties. Moreover, the self-diffusivity of R-32 and R-125 showed a linear increase with increasing solute concentration in the liquid phase (within the range of equilibrium pressures applied in this work) that affected more significantly (approximately 2-fold) to the smallest molecule R-32. This trend can be attributed to the fact that high pressures enhance the gas absorption, which increases the free volume of the solution. This leads to a reduction in the viscosity of the liquid phase, which in turn improves the transport properties of the solute [50]. However, it is important to note that a nonlinear relationship might be expected at higher pressures, as it happens with R-32 solubility in $[C_2C_1im][dca]$, which becomes slightly convex at pressures higher than 4 bar approximately [28]. For instance, Wang et al. [24] reported the self-diffusivity of neat R-32 and R-125 in $[C_4C_1im][BF_4]$ at 298.15 K and up to 10 bar, finding a logarithmic trend. Comparing both ILs, $[C_4C_1im][BF_4]$ and $[C_2C_1im][dca]$, there are significant differences in the viscosity and absorption capacity, and consequently in the solute self-diffusivities. For instance, at 3.70 bar, the mole fraction of R-32 in $[C_4C_1im][BF_4]$ was 0.25, with a self-diffusivity of $3.70 \times 10^{-10} \text{ m}^2 \text{ s}^{-1}$ [24]. In contrast, at a similar equilibrium pressure of 3.63 bar, the mole fraction of R-32 in $[C_2C_1im][dca]$ was 0.12, and its self-diffusivity was $5.43 \times 10^{-10} \text{ m}^2 \text{ s}^{-1}$. The major reason for this difference, despite the higher solubility of R-32 in $[C_4C_1im][BF_4]$, can be found in the viscosity

Table 6
Multicomponent self-diffusivity of R-32 and R-125, fed as R-410A blend, in $[\text{C}_2\text{C}_1\text{im}][\text{dca}]$ at 303.1 K and several pressures.^a

| $P_{\text{R-410A}}$ /bar | $P_{\text{R-32}}$ /bar | $D_{\text{R-32}} / 10^{-10} \text{ m}^2 \text{ s}^{-1}$ | $u(D_{\text{R-32}})$ | $P_{\text{R-125}}$ /bar | $D_{\text{R-125}} / 10^{-10} \text{ m}^2 \text{ s}^{-1}$ | $u(D_{\text{R-125}})$ |
|-----------------------------|------------------------|---|----------------------|-------------------------|--|-----------------------|
| 0.93 | 0.64 | 4.59 | 0.02 | 0.29 | 2.38 | 0.01 |
| 1.73 | 1.19 | 4.63 | 0.02 | 0.54 | 2.39 | 0.01 |
| 2.51 | 1.72 | 4.84 | 0.03 | 0.79 | 2.50 | 0.01 |
| 3.81 | 2.62 | 5.09 | 0.01 | 1.19 | 2.66 | 0.01 |

^a Standard uncertainties u are $u(T) = 0.1 \text{ K}$ and $u(P) = 0.01 \text{ bar}$.

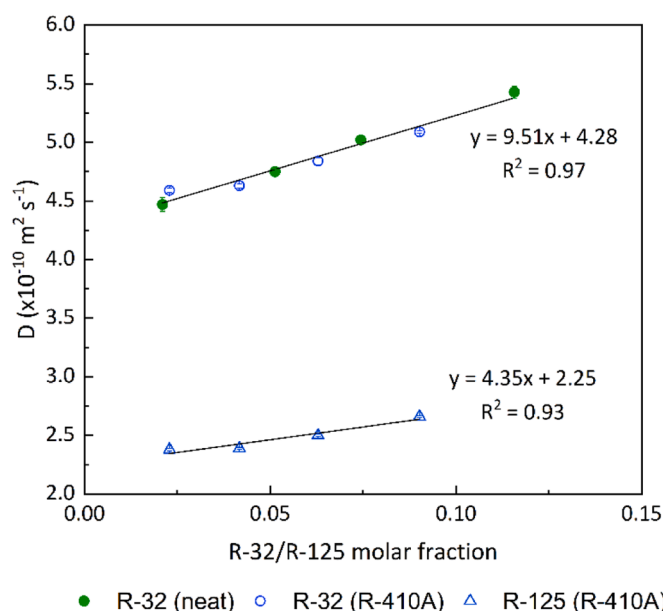


Fig. 5. Self-diffusivities of R-32 (circles) and R-125 (triangles) in $[\text{C}_2\text{C}_1\text{im}][\text{dca}]$ at 303.1 K as a function of the absorbed mole fraction. Filled and empty symbols correspond to pure R-32 and mixed R-410A feeds, respectively. Solid lines represent the linear regression of the data.

Table 7
Self-diffusivity of the $[\text{C}_2\text{C}_1\text{im}]^+$ and $[\text{dca}]^-$ ions in the absorption of pure R-32 at 303.1 K and several pressures.^a

| P /bar | $D_+ / 10^{-10} \text{ m}^2 \text{ s}^{-1}$ | $u(D_+)$ | $D_- / 10^{-10} \text{ m}^2 \text{ s}^{-1}$ | $u(D_-)$ |
|-------------|---|----------|---|----------|
| 0.00 | 1.25 | 0.04 | 1.47 | 0.02 |
| 0.66 | 1.30 | 0.02 | 1.52 | 0.02 |
| 1.62 | 1.43 | 0.07 | 1.67 | 0.01 |
| 2.45 | 1.46 | 0.05 | 1.72 | 0.01 |
| 3.63 | 1.57 | 0.05 | 1.85 | 0.02 |

^a Standard uncertainties u are $u(T) = 0.1 \text{ K}$ and $u(P) = 0.01 \text{ bar}$.

of the liquid phase, i.e., $[\text{C}_4\text{C}_1\text{im}][\text{BF}_4]$ is seven times more viscous than $[\text{C}_2\text{C}_1\text{im}][\text{dca}]$ at room temperature conditions.

Interestingly, a comparison between the self-diffusivity results (i.e., at constant chemical potential) of R-32 and R-125 obtained in this work and the Fickian diffusivity at infinite dilution (under a chemical potential gradient) reported by Asensio-Delgado et al. [28] for the same system are in quantitative agreement within the same order of magnitude. Although both diffusion coefficients are theoretically related [51], the difference observed can be attributed to the distinct nature of the data, as achieving an exact equivalence would require the absence of intermolecular interactions and similar molecular properties of the solute and solvent.

Table 8
Self-diffusivity of the $[\text{C}_2\text{C}_1\text{im}]^+$ and $[\text{dca}]^-$ ions in the absorption of R-410A at 303.1 K and several pressures.^a

| P/bar | $D_+ / 10^{-10} \text{ m}^2 \text{ s}^{-1}$ | $u(D_+)$ | $D_- / 10^{-10} \text{ m}^2 \text{ s}^{-1}$ | $u(D_-)$ |
|----------------|---|----------|---|----------|
| 0.00 | 1.25 | 0.04 | 1.47 | 0.02 |
| 0.93 | 1.32 | 0.08 | 1.57 | 0.01 |
| 1.73 | 1.38 | 0.04 | 1.64 | 0.02 |
| 2.51 | 1.42 | 0.03 | 1.65 | 0.01 |
| 3.81 | 1.49 | 0.04 | 1.78 | 0.02 |

^a Standard uncertainties u are $u(T) = 0.1 \text{ K}$ and $u(P) = 0.01 \text{ bar}$.

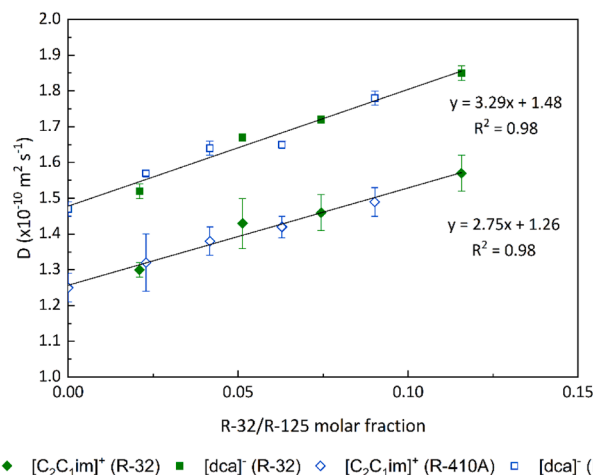


Fig. 6. Self-diffusivities of $[\text{C}_2\text{C}_1\text{im}]^+$ (diamonds) and $[\text{dca}]^-$ (squares) at equilibrium with either neat R-32 (filled symbols) or R-410A (empty symbols) at 303.1 K. Solid lines represent the linear regression of the $[\text{C}_2\text{C}_1\text{im}]^+$ and $[\text{dca}]^-$ self-diffusivities data from both sources. Molar fractions of gas absorbed taken from Tables 3 and 4.

3.3. IL self-diffusivity

The self-diffusion coefficients of the IL in the presence of R-32 and R-410A were also determined with ^{13}C PGSE NMR. The results are summarized in Tables 7 and 8. In all cases, the measured values of D_- were higher ($\sim 18\%$ on average) than those of D_+ , which can be related to the difference in the ions volume. Although $[\text{C}_2\text{C}_1\text{im}][\text{dca}]$ exhibits higher ionic dissociation than other conventional ILs [52], partial ion dissociation and aggregations due to interactions between ions and solute may occur. Thus, it should be taken into consideration that the NMR method would not distinguish between free and associated ion and, therefore, the self-diffusion coefficient of a cation and anion measured with NMR would represent respectively an average of the various cationic and anionic species present in the solution. The self-diffusivity values of $[\text{C}_2\text{C}_1\text{im}]^+$ are in very good agreement with those reported by Asensio-Delgado et al. [23] for a similar cyanide-based IL, with the

tricyanomethanide ([tcm]) anion, in the presence of other refrigerants, which were obtained from molecular dynamics trajectories.

In addition, Fig. 6 represents the self-diffusivity of the cation and anion moieties as a function of the mole fraction of absorbed gas for both feeds, i.e., the neat R-32 and the R-410A mixture. The diffusion coefficients of both ions also increased with increasing concentration of sorbed gases, yet less significantly than for the refrigerants. As previously stated, this can be mainly due to a decrease of the viscosity of the medium, as it is generally found in mixtures of fluorinated gases with ILs [9,10]. Regarding the influence of the feed source, the self-diffusivity of the cation and anion exhibited a consistent pattern when in contact with either R-32 or R-410A. Therefore, the effect of R-125 on IL self-diffusivity was practically negligible. This phenomenon could be attributed to the reduced absorption of R-125 in the IL, minimizing its impact. It should be pointed out that the study was performed with a discrete set of pressure and temperature values because of current technical limitations at our laboratory. Nevertheless, hardware to enable measurements with a wider range of those variables could be obtained.

4. Conclusions

In this work, the solubility and self-diffusivity of the neat refrigerant R-32 and the mixture R-410A in the IL [C₂C₁im][dca] were measured with NMR spectroscopy and PGSE NMR techniques at several pressures and 303.1 K. The simultaneous self-diffusivity results of a commercial mixture of HFCs in IL media are shown for the first time, showing the potential of NMR techniques for the fast and reliable assessment of transport properties of fluorinated gases and ILs systems. The solubility results did not show any notable mixing effect, indicating that the solubility of R-32 and R-125 were essentially equivalent for both the pure compound and the R-410A mixture, within the investigated pressure range. This behaviour was also reflected in the results of the self-diffusivity measurements. In addition, the self-diffusivity values increased with the mole fraction of the absorbed gas. This effect can be attributed to a reduction in the viscosity of the medium, which enhanced the mass transport phenomena. Overall, NMR allowed obtaining valuable knowledge on the equilibrium and transport properties of multi-component systems for the design of efficient and sustainable separation processes for the recycling of value-added HFCs in the refrigeration sector.

CRedit authorship contribution statement

Miguel Viar: Writing – original draft, Investigation, Formal analysis. **Fernando Pardo:** Formal analysis. **Gabriel Zarca:** Writing – review & editing, Funding acquisition, Formal analysis, Conceptualization. **Leoncio Garrido:** Writing – original draft, Resources, Methodology, Investigation, Formal analysis. **Ane Urtiaga:** Writing – review & editing, Funding acquisition, Formal analysis, Conceptualization.

Declaration of competing interest

The authors declare that they have no known competing financial interests or personal relationships that could have appeared to influence the work reported in this paper.

Acknowledgements

The authors acknowledge the financial support of MICIU/AEI/10.13039/501100011033 and the European Union NextGenerationEU/PRTR to projects TED2021-129844B-I00 and PID2022-138028OB-I00 (Universidad de Cantabria), and project PID2019-108552GB-I00 (ICTP-CSIC) as well as project LIFE4F-Gases (LIFE20CCM/ES/001748) co-funded by the European Union LIFE programme. F. Pardo thanks the postdoctoral fellowship IJC2020-043134-I “Juan de la Cierva Incorporación”. M. Viar acknowledges the FPU grant (FPU22/04137) awarded

by the Spanish Ministry of Education and Professional Training.

Data availability

The manuscript reports all the research data

References

- [1] N.D. Miranda, P. Giovani Palafox-Alcantar, R. Khosla, M.D. McCulloch, Metrics for the emissions of F-gas refrigerants, *Sustain. Energy Technol. Assessments* 58 (2023) 103348, <https://doi.org/10.1016/j.seta.2023.103348>.
- [2] A. Mota-Babiloni, J. Navarro-Esbrí, A. Barragán-Cervera, F. Molés, B. Peris, Analysis based on EU Regulation No 517/2014 of new HFC/HFO mixtures as alternatives of high GWP refrigerants in refrigeration and HVAC systems, *Int. J. Refrig.* 52 (2015) 21–31, <https://doi.org/10.1016/j.ijrefrig.2014.12.021>.
- [3] A. Mota-Babiloni, P. Makhnatch, Predictions of European refrigerants place on the market following F-gas regulation restrictions, *Int. J. Refrig.* 127 (2021) 101–110, <https://doi.org/10.1016/j.ijrefrig.2021.03.005>.
- [4] M.O. McLinden, M.L. Huber, (R)Evolution of refrigerants, *J. Chem. Eng. Data* 65 (2020) 4176–4193, <https://doi.org/10.1021/acs.jced.0c00338>.
- [5] R. Ciconkov, Refrigerants: there is still no vision for sustainable solutions, *Int. J. Refrig.* 86 (2018) 441–448, <https://doi.org/10.1016/j.ijrefrig.2017.12.006>.
- [6] F. Graziosi, J. Arduini, F. Furlani, U. Giostra, P. Cristofanelli, X. Fang, O. Hermanssen, C. Lunder, G. Maenhout, S. O’Doherty, S. Reimann, N. Schmidbauer, M.K. Vollmer, D. Young, M. Maione, European emissions of the powerful greenhouse gases hydrofluorocarbons inferred from atmospheric measurements and their comparison with annual national reports to UNFCCC, *Atmos. Environ.* 158 (2017) 85–97, <https://doi.org/10.1016/j.atmosenv.2017.03.029>.
- [7] Y. Heredia-Aricapa, J.M. Belman-Flores, A. Mota-Babiloni, J. Serrano-Arellano, J. J. García-Pabón, Overview of low GWP mixtures for the replacement of HFC refrigerants: r134a, R404A and R410A, *Int. J. Refrig.* 111 (2020) 113–123, <https://doi.org/10.1016/j.ijrefrig.2019.11.012>.
- [8] C.G. Albà, I.L.I. Alkhatib, F. Llovel, L.F. Vega, Assessment of low global warming potential refrigerants for drop-in replacement by connecting their molecular features to their performance, *ACS Sustain. Chem. Eng.* 9 (2021) 17034–17048, <https://doi.org/10.1021/acssuschemeng.1c05985>.
- [9] K.R. Baca, K. Al-Barghouti, N. Wang, M.G. Bennett, L.M. Valenciano, T.L. May, I. V. Xu, M. Cordry, D.M. Haggard, A.G. Haas, A. Heimann, A.N. Harders, H.G. Uhl, D.T. Melfi, A.D. Yancey, R. Kore, E.J. Maginn, A.M. Scurto, M.B. Shiflett, Ionic liquids for the separation of fluorocarbon refrigerant mixtures, *Chem. Rev.* 124 (2024) 5167–5226, <https://doi.org/10.1021/acs.chemrev.3c00276>.
- [10] S. Asensio-Delgado, F. Pardo, G. Zarca, A. Urtiaga, Absorption separation of fluorinated refrigerant gases with ionic liquids: equilibrium, mass transport, and process design, *Sep. Purif. Technol.* 276 (2021) 119363, <https://doi.org/10.1016/j.seppur.2021.119363>.
- [11] M. Viar, S. Asensio-Delgado, F. Pardo, G. Zarca, A. Urtiaga, In the quest for ionic liquid entrainers for the recovery of R-32 and R-125 by extractive distillation under rate-based considerations, *Sep. Purif. Technol.* 324 (2023) 124610, <https://doi.org/10.1016/j.seppur.2023.124610>.
- [12] M.S. Monjur, A. Iftakher, M.M.F. Hasan, Separation process synthesis for high-GWP refrigerant mixtures: extractive distillation using ionic liquids, *Ind. Eng. Chem. Res.* 61 (2022) 4390–4406, <https://doi.org/10.1021/acs.iecr.2c00136>.
- [13] E.A. Finberg, T.L. May, M.B. Shiflett, Multicomponent refrigerant separation using extractive distillation with ionic liquids, *Ind. Eng. Chem. Res.* 61 (2022) 9795–9812, <https://doi.org/10.1021/acs.iecr.2c00937>.
- [14] M.B. Shiflett, A. Yokozeki, Solubility and diffusivity of hydrofluorocarbons in room-temperature ionic liquids, *AIChE J.* 52 (2006) 1205–1219, <https://doi.org/10.1002/aic.10685>.
- [15] K.S. Al-Barghouti, K.R. Baca, M.B. Shiflett, A.M. Scurto, Phase equilibrium and transport properties of the ionic liquid 1-Ethyl-3-methylimidazolium Bis (trifluoromethylsulfonyle)amide and compressed difluoromethane and pentafluoroethane, *Ind. Eng. Chem. Res.* 63 (2024) 1151–1169, <https://doi.org/10.1021/acs.iecr.3c03491>.
- [16] S. Asensio-Delgado, F. Pardo, G. Zarca, A. Urtiaga, Enhanced absorption separation of hydrofluorocarbon/hydrofluoroolefin refrigerant blends using ionic liquids, *Sep. Purif. Technol.* 249 (2020) 117136, <https://doi.org/10.1016/j.seppur.2020.117136>.
- [17] M. Viar, S. Asensio-Delgado, F. Pardo, G. Zarca, A. Urtiaga, Solubility of difluoromethane (R-32) and pentafluoroethane (R-125) in 1-alkyl-3-methylimidazolium tricyanomethanide ionic liquids, *Fluid Phase Equilib.* 577 (2024) 113983, <https://doi.org/10.1016/j.fluid.2023.113983>.
- [18] S. Asensio-Delgado, F. Pardo, G. Zarca, A. Urtiaga, Machine learning for predicting the solubility of high-GWP fluorinated refrigerants in ionic liquids, *J. Mol. Liq.* (2022) 120472, <https://doi.org/10.1016/j.molliq.2022.120472>.
- [19] J. Chu, M. He, G.M. Kontogeorgis, X. Liu, X. Liang, Screening HFC/HFO and ionic liquid for absorption refrigeration at the atomic scale by the prediction model of machine learning, *Green Chem. Eng.* (2024), <https://doi.org/10.1016/j.gce.2024.07.004>.
- [20] J.E. Sosa, R. Santiago, A.E. Redondo, J. Avila, L.F. Lepre, M.C. Gomes, J.M. Araujo, J. Palomar, A.B. Pereiro, Design of ionic liquids for fluorinated gas absorption: COSMO-RS selection and solubility experiments, *Environ. Sci. Technol.* 56 (2022) 5898–5909, <https://doi.org/10.1021/acs.est.2c00051>.

- [21] R. Santiago, I. Díaz, M. González-Miquel, P. Navarro, J. Palomar, Assessment of bio-ionic liquids as promising solvents in industrial separation processes: computational screening using COSMO-RS method, *Fluid Phase Equilib.* 560 (2022), <https://doi.org/10.1016/j.fluid.2022.113495>.
- [22] H. Qin, J. Cheng, H. Yu, T. Zhou, Z. Song, Hierarchical ionic liquid screening integrating COSMO-RS and aspen plus for selective recovery of hydrofluorocarbons and hydrofluoroolefins from a refrigerant blend, *Ind. Eng. Chem. Res.* 61 (2022) 4083–4094, <https://doi.org/10.1021/acs.iecr.1c04688>.
- [23] S. Asensio-Delgado, M. Viar, A.A.H. Pádua, G. Zarca, A. Urriaga, Understanding the molecular features controlling the solubility differences of R-134a, R-1234ze(E), and R-1234yf in 1-Alkyl-3-methylimidazolium tricyanomethanide ionic liquids, *ACS Sustain. Chem. Eng.* 10 (2022) 15124–15134, <https://doi.org/10.1021/acssuschemeng.2c04561>.
- [24] N. Wang, Y. Zhang, K.S. Al-Barghouti, R. Kore, A.M. Scurto, E.J. Maginn, Structure and dynamics of hydrofluorocarbon/ionic liquid mixtures: an experimental and molecular dynamics study, *J. Phys. Chem. B* 126 (2022) 8309–8321, <https://doi.org/10.1021/acs.jpcc.2c05787>.
- [25] K.R. Baca, D.P. Broom, M.G. Roper, M.J. Benham, M.B. Shiflett, First Measurements for the simultaneous sorption of difluoromethane and pentafluoroethane mixtures in ionic liquids using the integral mass balance method, *Ind. Eng. Chem. Res.* 61 (2022) 9774–9784, <https://doi.org/10.1021/acs.iecr.2c00497>.
- [26] A. Ifakher, T. Leonard, M.M.F. Hasan, Integrating different fidelity models for process optimization: a case of equilibrium and rate-based extractive distillation using ionic liquids, *Comput. Chem. Eng.* (2024) 108890, <https://doi.org/10.1016/j.compchemeng.2024.108890>.
- [27] X. Liu, P. Pan, M. He, Vapor-liquid equilibrium and diffusion coefficients of R32 + [HMIM][FEP], R152a + [HMIM][FEP] and R161 + [HMIM][FEP], *J. Mol. Liq.* 253 (2018) 28–35, <https://doi.org/10.1016/j.molliq.2018.01.032>.
- [28] S. Asensio-Delgado, M. Viar, F. Pardo, G. Zarca, A. Urriaga, Gas solubility and diffusivity of hydrofluorocarbons and hydrofluoroolefins in cyanide-based ionic liquids for the separation of refrigerant mixtures, *Fluid Phase Equilib.* 549 (2021) 113210, <https://doi.org/10.1016/j.fluid.2021.113210>.
- [29] S. Asensio-Delgado, F. Pardo, G. Zarca, A. Urriaga, Vapor–liquid equilibria and diffusion coefficients of difluoromethane, 1,1,1,2-tetrafluoroethane, and 2,3,3,3-Tetrafluoropropene in Low-Viscosity Ionic Liquids, *J. Chem. Eng. Data* 65 (2020) 4242–4251, <https://doi.org/10.1021/acs.jced.0c00224>.
- [30] A.R.C. Morais, A.N. Harders, K.R. Baca, G.M. Olsen, B.J. Befort, A.W. Dowling, E. J. Maginn, M.B. Shiflett, Phase equilibria, diffusivities, and equation of state modeling of HFC-32 and HFC-125 in imidazolium-based ionic liquids for the separation of R-410A, *Ind. Eng. Chem. Res.* 59 (2020) 18222–18235, <https://doi.org/10.1021/acs.iecr.0c02820>.
- [31] K.R. Baca, G.M. Olsen, L.M. Valenciano, M.G. Bennett, D.M. Haggard, B.J. Befort, A. Garcíadiego, A.W. Dowling, E.J. Maginn, M.B. Shiflett, Phase equilibria and diffusivities of HFC-32 and HFC-125 in ionic liquids for the separation of R-410A, *ACS Sustain. Chem. Eng.* 10 (2022) 816–830, <https://doi.org/10.1021/acssuschemeng.1c06252>.
- [32] L. Garrido, C. García, M. López-González, B. Comesaña-Gándara, Á.E. Lozano, J. Guzmán, Determination of gas transport coefficients of mixed gases in 6FDA-TMPDA polyimide by NMR Spectroscopy, *Macromolecules* 50 (2017) 3590–3597, <https://doi.org/10.1021/acs.macromol.7b00384>.
- [33] K. Damodaran, Recent advances in NMR spectroscopy of ionic liquids, *Prog. Nucl. Magn. Reson. Spectrosc.* 129 (2022) 1–27, <https://doi.org/10.1016/j.pnmrs.2021.12.001>.
- [34] E.O. Stejskal, J.E. Tanner, Spin diffusion measurements: spin echoes in the presence of a time-dependent field gradient, *J. Chem. Phys.* 42 (1965) 288–292, <https://doi.org/10.1063/1.1695690>.
- [35] A. Noda, K. Hayamizu, M. Watanabe, Pulsed-gradient spin-echo 1H and 19F NMR ionic diffusion coefficient, viscosity, and ionic conductivity of non-chloroaluminate room-temperature ionic liquids, *J. Phys. Chem. B* 105 (2001) 4603–4610, <https://doi.org/10.1021/jp004132q>.
- [36] M. Anouti, J. Jacquemin, P. Porion, Transport properties investigation of aqueous protic ionic liquid solutions through conductivity, viscosity, and NMR self-diffusion measurements, *J. Phys. Chem. B* 116 (2012) 4228–4238, <https://doi.org/10.1021/jp3010844>.
- [37] O. Nordness, J.F. Brennecke, Ion dissociation in ionic liquids and ionic liquid solutions, *Chem. Rev.* 120 (2020) 12873–12902, <https://doi.org/10.1021/acs.chemrev.0c00373>.
- [38] P.T. Callaghan, *Translational Dynamics & Magnetic Response. Principles of Pulsed Gradient Spin Echo NMR*, Oxford University Press, 2011, <https://doi.org/10.1093/acprof:oso/9780199556984.001.0001>.
- [39] W.S. Price, *NMR Studies of Translational Motion Hardback: Principles and Applications*, Cambridge University Press, 2009.
- [40] D.S. Grebenkov, *From the microstructure to diffusion NMR, and back. Diffusion NMR of Confined Systems: Fluid Transport In Porous Solids and Heterogeneous Materials*, The Royal Society of Chemistry, 2017, pp. 52–110.
- [41] A. Hosseini, W. Ren, L.R. Weatherley, A.M. Scurto, Viscosity and self-diffusivity of ionic liquids with compressed hydrofluorocarbons: 1-Hexyl-3-methyl-imidazolium bis(trifluoromethylsulfonyl)amide and 1,1,1,2-tetrafluoroethane, *Fluid Phase Equilib.* 437 (2017) 34–42, <https://doi.org/10.1016/j.fluid.2016.11.022>.
- [42] J. Guzmán, L. Garrido, Determination of carbon dioxide transport coefficients in liquids and polymers by NMR spectroscopy, *J. Phys. Chem. B* 116 (2012) 6050–6058, <https://doi.org/10.1021/jp302037w>.
- [43] L. Garrido, J. Guzmán, Influence of diffusion time on the diffusion coefficients of gases in polymers determined by pulsed gradient spin echo NMR, *Macromolecules* 51 (2018) 8681–8688, <https://doi.org/10.1021/acs.macromol.8b02107>.
- [44] A.P. Carneiro, C. Held, O. Rodríguez, G. Sadowski, E.A. Macedo, Solubility of sugars and sugar alcohols in ionic liquids: measurement and PC-SAFT modeling, *J. Phys. Chem. B* 117 (2013) 9980–9995, <https://doi.org/10.1021/jp404864c>.
- [45] P. Wächter, C. Schreiner, H.G. Schweiger, H.J. Gores, Determination of phase transition points of ionic liquids by combination of thermal analysis and conductivity measurements at very low heating and cooling rates, *J. Chem. Thermodyn.* 42 (2010) 900–903, <https://doi.org/10.1016/j.jct.2010.03.003>.
- [46] Y. Zheng, Y. Zheng, Q. Wang, Z. Wang, Density, viscosity, and electrical conductivity of 1-Alkyl-3-methylimidazolium dicyanamide ionic liquids, *J. Chem. Eng. Data* 66 (2021) 480–493, <https://doi.org/10.1021/acs.jced.0c00754>.
- [47] J.E. Tanner, Use of the stimulated echo in NMR diffusion studies, *J. Chem. Phys.* 52 (1970) 2523–2526, <https://doi.org/10.1063/1.1673336>.
- [48] O. Söderman, W.S. Price, M. Schönhoff, D. Topgaard, NMR diffusometry applied to liquids, *J. Mol. Liq.* 156 (2010) 38–44, <https://doi.org/10.1016/j.molliq.2010.05.007>.
- [49] L. Garrido, M. López-González, E. Saiz, E. Riande, Molecular basis of carbon dioxide transport in polycarbonate membranes, *J. Phys. Chem. B* 112 (2008) 4253–4260, <https://doi.org/10.1021/jp711080h>.
- [50] D.L. Minnick, M.B. Shiflett, Solubility and diffusivity of chlorodifluoromethane in imidazolium ionic liquids: [emim][Tf2N], [bmim][BF4], [bmim][PF6], and [emim][TFES], *Ind. Eng. Chem. Res.* 58 (2019) 11072–11081, <https://doi.org/10.1021/acs.iecr.9b02419>.
- [51] K. Malek, M.O. Coppens, Knudsen self- and Fickian diffusion in rough nanoporous media, *J. Chem. Phys.* 119 (2003) 2801–2811, <https://doi.org/10.1063/1.1584652>.
- [52] Y. Zheng, Y. Zheng, Q. Wang, Z. Wang, Density, viscosity, and electrical conductivity of 1-alkyl-3-methylimidazolium dicyanamide ionic liquids, *J. Chem. Eng. Data* 66 (2021) 480–493, <https://doi.org/10.1021/acs.jced.0c00754>.